

Topography of Nicotinic Acetylcholine Receptor Membrane-embedded Domains*

Received for publication, June 16, 2000, and in revised form, August 30, 2000
Published, JBC Papers in Press, August 30, 2000, DOI 10.1074/jbc.M005246200

Francisco J. Barrantes‡§, Silvia S. Antollini‡, Michael P. Blanton¶, and Manuel Prieto||

From the ‡Instituto de Investigaciones Bioquímicas de Bahía Blanca, B8000FWB Bahía Blanca, Argentina, the ¶Departments of Pharmacology and Anesthesiology, Texas Tech University, Health Sciences Center, Lubbock, Texas 79430, and the ||Centro de Química-Física Molecular, Complexo Interdisciplinar, 1049-001 Lisboa, Portugal

The topography of nicotinic acetylcholine receptor (AChR) membrane-embedded domains and the relative affinity of lipids for these protein regions were studied using fluorescence methods. Intact *Torpedo californica* AChR protein and transmembrane peptides were derivatized with *N*-(1-pyrenyl)maleimide (PM), purified, and reconstituted into asolectin liposomes. Fluorescence mapped to proteolytic fragments consistent with PM labeling of cysteine residues in α M1, α M4, γ M1, and γ M4. The topography of the pyrene-labeled Cys residues with respect to the membrane and the apparent affinity for representative lipids were determined by differential fluorescence quenching with spin-labeled derivatives of fatty acids, phosphatidylcholine, and the steroids cholesterol and androstane. Different spin label lipid analogs exhibit different selectivity for the whole AChR protein and its transmembrane domains. In all cases labeled residues were found to lie in a shallow position. For M4 segments, this is compatible with a linear α -helical structure, but not so for M1, for which "classical" models locate Cys residues at the center of the hydrophobic stretch. The transmembrane topography of M1 can be rationalized on the basis of the presence of a substantial amount of non-helical structure, and/or of kinks attributable to the occurrence of the evolutionarily conserved proline residues. The latter is a striking feature of M1 in the AChR and all members of the rapid ligand-gated ion channel superfamily.

The muscle and electric organ nicotinic acetylcholine receptor (AChR)¹ is a pentameric integral transmembrane protein of homologous $\alpha_2\beta\gamma\delta$ subunits. The AChR belongs to a superfamily

of ligand-gated ion channels, together with the glycine receptor, a subtype of the serotonin receptor (5-HT₃), and the GABA_A receptor (1–4). Each AChR subunit contains a relatively large amino-terminal extracellular domain of ~200 amino acids followed by four hydrophobic domains of 20–30 amino acids in length (M1–M4) connected by hydrophilic loops of varying length and ending with a very short extracellular carboxyl terminus (reviewed in Ref. 5).

Although the exact topology of the AChR relative to the membrane has not yet been determined unambiguously, it is usually accepted that the four hydrophobic segments M1–M4 correspond to transmembrane (TM) domains (6–7). There is still contradictory evidence on their secondary structure. The original postulation of a four-helix bundle with an all-helical secondary structure (8) has been challenged by the results of cryoelectron microscopy of frozen AChR tubules (9–10) and computer-aided molecular modeling indicating that the dimensions of the AChR TM region are not compatible with a pentameric four-helix bundle (11). Site-directed mutagenesis data combined with patch clamp electrophysiology, and results from photoaffinity labeling with noncompetitive channel blockers, support the notion that the M2 domain lines the walls of the ion channel proper and are indicative of α -helical periodicity in the residues exposed to the lumen of the channel (4). Recent NMR spectroscopy studies of the δ M2 segment (12), indicate that this domain is inserted in the bilayer at an angle of 12° relative to the membrane normal, with no kinks, and in totally α -helical configuration. A synthetic peptide corresponding to the *Torpedo* α M2 segment in chloroform:methanol containing LiClO₄ also adopts a totally α -helical configuration (13).

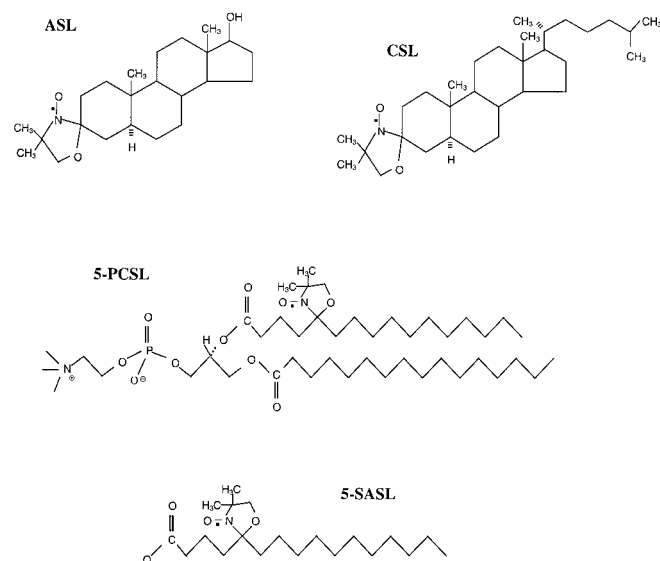
The cryoelectron microscopy studies are further interpreted to indicate that the other putative TM domains (M1, M3, and M4) are relatively featureless, with a large portion of the polypeptide chain in an extended (or unresolved) β -sheet configuration, arranged in the form of a large β -barrel outside the central rim of M2 channel-forming rods (9–10). This interpretation is in contrast to the studies using photoactivatable hydrophobic probes, in which the observed periodicity of the lipid-exposed residues in M4 and M3 is consistent with an α -helical pattern (6, 14, 15) and with deuterium-exchange FTIR studies which indicate a predominantly α -helical structure in the AChR TM region (16). In addition, secondary structure analysis (CD and FTIR spectroscopy) of isolated and lipid-reconstituted TM AChR peptides indicate α -helical structure for M2, M3, and M4 segments (17). Furthermore, two-dimensional ¹H NMR spectroscopy of a synthetic peptide corresponding to the α M3 segment of *Torpedo* AChR showed a totally α -helical structure (18), and a recent NMR study of a synthetic

fluoromethyl-3-[¹²⁵I]iodophenyldiazirine; FTIR, Fourier transform infrared spectroscopy.

* This work was supported in part by grants from the Universidad Nacional del Sur, the Agencia Nacional de Promoción Científica, Argentina, the Commission of Scientific Investigations of the Province of Buenos Aires (CIC), FIRCA 1-RO3-TW01225-01 and Antorchas/British Council (to F. J. B.), National Institute of Neurological Disorders and Stroke Grant R29 NS35786 (to M. P. B.), and the ICITI, Instituto de Cooperação Científica e Tecnológica and FCT Fundação para a Ciência e Tecnologia (Portugal) (to M. P.). The costs of publication of this article were defrayed in part by the payment of page charges. This article must therefore be hereby marked "advertisement" in accordance with 18 U.S.C. Section 1734 solely to indicate this fact.

§ To whom correspondence should be addressed: Instituto de Investigaciones Bioquímicas de Bahía Blanca, C. C. 857, B8000BZW Bahía Blanca, Argentina. Tel.: 54-291-486-1201; Fax: 54-291-486-1200; E-mail: rtfjb1@criba.edu.ar.

¹ The abbreviations used are: AChR, nicotinic acetylcholine receptor; ASL, 3-doxy-17 β -hydroxy-5 α -androstane spin label; CSL, 3 β -doxy-5 α -cholestanol spin label; 5-SASL, 5-doxy-17 β -hydroxy-5 α -androstane spin label; 7-SASL, 7-doxy-17 β -hydroxy-5 α -androstane spin label; 12-PCSL, 12-doxy-17 β -hydroxy-5 α -androstane spin label; 12-SASL, 12-doxy-17 β -hydroxy-5 α -androstane spin label; PM, *N*-(1-pyrenyl)-maleimide; TM, transmembrane; HPLC, high performance liquid chromatography; PAGE, polyacrylamide gel electrophoresis; Tricine, *N*-[2-hydroxy-1,1-bis(hydroxymethyl)ethyl]glycine; TID, 3-tri-



SCHEME I. Structural formulas of the spin-labeled probes used in this study.

γ M4 peptide is also compatible with an α -helical secondary structure (19).

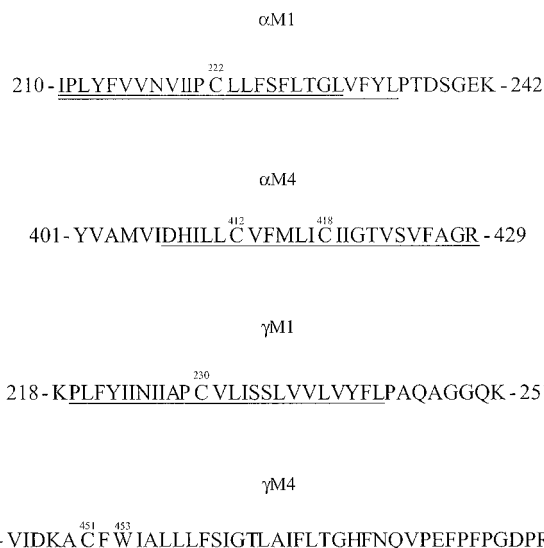
In the present work the spatial relationship between membrane-embedded domains of the *Torpedo californica* AChR and the membrane bilayer was studied using fluorescence spectroscopy. The location of the pyrene-labeled cysteine residues with respect to the membrane was determined by differential quenching with spin-labeled lipids. Both in intact AChR and in reconstituted individual TM peptides, Cys residues were located close to the membrane-water interface, as predicted for the segments α M4 and γ M4 (6, 14, 15). In the case of M1 segments, our fluorescence studies indicate that these membrane-embedded domains are not a straight α -helix and/or possess pronounced kinks. Our observations lend support to the hypothesis that M1 membrane-embedded domains in general depart from linear structures, thus extending the conclusion of cysteine-scanning mutagenesis (20), fluorescence (21), and CD and FTIR spectroscopy (17) studies on α M1.

EXPERIMENTAL PROCEDURES

Materials—The spin-labeled fatty acids, derived from the stearic acid substituted on positions 5 (5-SASL, 5-doxy-stearic acid), 7 (7-SASL, 7-doxy-stearic acid), and 12 (12-SASL, 12-doxy-stearic acid), and the equivalent phosphatidylcholine derivative 12-PCSL, were obtained from Avanti Polar Lipids, Birmingham, AL. Nitroxide-labeled CSL (3 β -doxyl-5 α -cholestane spin label) and 3-doxy-17 β -hydroxy-5 α -androstane spin label (ASL) were from Aldrich Chemical Co., and used as received. The formula of the spin-labeled lipid analogs are shown in Scheme I.

Pyrene maleimide (PM) was obtained from Molecular Probes and [¹²⁵I]TID (10 Ci/mmol) from Amersham Pharmacia Biotech. Affi-Gel 10 was purchased from Bio-Rad, Genapol C-100 (10%) from Calbiochem, and sodium cholate from Sigma. Asolectin, a crude soybean lipid extract, came from Avanti Polar Lipids and Spectra/Por Dispo Dialyzers (molecular mass cutoff: 2,000 Da) from Spectrum.

Affinity Column Purification of AChR Labeled with PM and Reconstituted into Lipid Vesicles—AChR-rich membranes were isolated from the electric organ of *T. californica* (Aquatic Research Consultants, San Pedro, CA) according to the procedure of Sobel *et al.* (22), with the modifications described previously (23). The final membrane suspensions in ~36% sucrose/0.02% NaN₃ were stored at -80 °C. The *Torpedo* AChR was solubilized in 1% sodium cholate, and PM (2 mM) was allowed to react with available cysteine residues (1 h incubation). The labeled AChR (PM-labeled AChR) was purified by affinity chromatography in the presence of asolectin lipids. Affinity column purification was performed using an acetylcholine affinity matrix (24) with a number of modifications (25). Briefly, the affinity column matrix was prepared by coupling cystamine to Affi-Gel 10 (Bio-Rad), reduction with



SCHEME II. *T. californica* AChR transmembrane peptides. The transmembrane region of α M1 is indicated by the shorter line according to Ref. 21 and by the longer line according to Ref. 19. For the other fragments the extension of the transmembrane domains are taken from Ref. 19.

dithiothreitol, and final modification with bromoacetylcholine bromide. Affinity purified PM-AChRs were reconstituted with asolectin at a lipid:protein ratio of 800:1 on a mol/mol basis and stored at -80 °C. The ability of PM-AChR to undergo agonist-induced conformational transitions was verified by examining the extent of [¹²⁵I]TID photoincorporation into PM-AChR subunits in the absence and presence of agonist. The amount of [¹²⁵I]TID photoincorporation into AChR subunits is ~10-fold greater in the resting state AChR than in the desensitized state and therefore [¹²⁵I]TID subunit labeling is an extremely sensitive indicator of the conformational state of the AChR as well as of agonist-induced state transitions (26, 27).

Isolation and Reconstitution of Proteolytic Fragments of AChR Subunits Containing PM-labeled Transmembrane Segments—Proteolytic fragments of AChR subunits which contain the M1 or M4 transmembrane segment of the α - and γ -subunit were prepared as described in Corbin *et al.* (17). Each TM peptide contains either a single cysteine residue (α M1, γ M1, and γ M4) or two cysteine residues (α M4), as shown in Scheme II. The isolated fragments in 0.1% sodium dodecyl sulfate were reacted with pyrene maleimide (3 mM) overnight. The PM-labeled peptides were purified by reverse-phase HPLC using a Brownlee Aquapore C₄ column (100 \times 2.1 mm). Solvent A was 0.08% trifluoroacetic acid in water, and solvent B was 0.05% trifluoroacetic acid in 60% acetonitrile, 40% 2-propanol. The flow rate was maintained at 0.2 ml/min and 0.5-ml fractions were collected. Peptides were eluted with a nonlinear gradient from 25 to 100% solvent B in 80 min. The elution of peptides was monitored by the absorbance at 210 nm as well as by fluorescence emission (350 nm excitation, 400 nm emission).

Peptide-containing HPLC fractions were pooled and dried by vacuum centrifugation. Peptides were resuspended in 1 ml of 2% octyl- β -glucoside and asolectin lipid in 2% sodium cholate was added to achieve an estimated lipid to peptide molar ratio of ~200:1. The octyl- β -glucoside and sodium cholate were removed by dialysis using Spectra/Por CE Dispo Dialyzers with a 2000 *M_r* cutoff, for 2 days against phosphate buffer (10 mM phosphate, 5 mM NaCl, pH 7.0). Each sample was concentrated to 200 μ l using a Centricon-3 and stored at -80 °C. A small aliquot of each sample was subjected to NH₂-terminal amino acid sequence analysis in order to confirm the identity of the peptide and estimate its concentration (α M1, Ile²¹⁰-Lys²⁴²; α M4, Val⁴⁰¹-Arg⁴²⁸; γ M1, Lys²¹⁸-Lys²⁵¹; γ M4, Val⁴⁴⁶-Arg⁴⁸⁵). An additional aliquot was labeled with the hydrophobic photoreagent [¹²⁵I]TID. The labeled peptide was resolved on a 1.0-mm thick Tricine gel (28) and the dried gel subjected to autoradiography. Labeling with [¹²⁵I]TID served as an additional test of peptide purity and to confirm that no significant peptide aggregation (irreversible) had occurred.

Sequence Analysis—Amino-terminal sequence analysis was performed on a Beckman Instruments (Porton) Model 20/20 protein sequencer using gas phase cycles (Texas Tech Biotechnology Core Facility). Peptide aliquots (~10 μ l) were immobilized on chemically modified glass fiber discs (Beckman Instruments), which were used to improve

the sequencing yields of hydrophobic peptides. Peptides were subjected to 10 sequencing cycles and initial yield (I_0) and repetitive yield (R) were calculated by nonlinear least square regression of the observed release (M) for each cycle (n): $M = I_0 R^n$.

Fluorescence Measurements—These were carried out using an SLM model 4800 spectrofluorimeter (SLM Instruments, Urbana, IL) with its cuvette holder thermostated at 20 °C. Whole PM-labeled AChR reconstituted in asolectin was made to a final concentration of 0.05 μM in 5×5 -mm quartz cuvettes. Fluorescence quenching was carried out with nitroxide spin-labeled phosphatidylcholine (12-PCSL), spin-labeled cholestane (CSL), and androstane (ASL), and the spin-labeled stearic acid analogs 5-SASL, 7-SASL, and 12-SASL. The highest nitroxide concentration employed was 24 μM . Lipid concentration was kept at 37 μM . In the case of PM-labeled AChR peptide fragments, they were resuspended at a final concentration of 0.05 μM . Lipid concentration was 8 μM . Titration with spin-labeled probes was made up to a final concentration of 8 μM . Pyrene was excited at $\lambda_{\text{exc}} = 345$ nm and its emission was monitored at $\lambda_{\text{em}} = 382$ nm. Slits of 5 nm were used in both monochromators.

Relevant corrections were taken into account, as follows: (i) inner filter effect due to the quencher absorption. The nitroxide labels used have a weak absorption in the UV, $\lambda_{430\text{ nm}} = 14 \text{ M}^{-1} \text{ cm}^{-1}$ (29). From the absorption tail a value of $E = 100 \text{ M}^{-1}$ at the pyrene excitation wavelength ($\lambda_{\text{exc}} = 345$ nm) is determined. The molar absorptivity of pyrene is 38,000 (30). From Equation 1 the correction factor C for the fluorescence intensity is obtained as,

$$C = (A_{\text{total}}/A_f) \times ((1 - 10^{-A_f})/(1 - 10^{-A_{\text{total}}})) \quad (\text{Eq. 1})$$

where A_f is the pyrenyl absorption and A_{total} the absorption of both PM-labeled AChR (or peptide) and nitroxide spin label. Under the experimental conditions used, this factor amounts to only 0.2% for the highest concentration of nitroxide used. (ii) Effective quencher concentration in the membrane. The determination of effective spin label concentrations in the membrane volume $[Q]_L$, should take into account the different incorporation of the various fatty acid probes in the bilayer described by its partition constant K_p . This was carried out using the relationship (31),

$$[Q]_L = (K_p/(1 + (K_p - 1) \gamma_L * [L])) * [Q]_T \quad (\text{Eq. 2})$$

where γ_L is the lipid molar volume and $[Q]_T$ the analytical quencher concentration. The partition constants used for the spin-labeled fatty acids are: 9.6×10^4 (5-SASL), 9.8×10^4 (7-SASL), and 2.9×10^4 (12-SASL) (32). These values are reported for a lipid system also in the fluid phase (egg phosphatidylcholine), and at 25 °C, a temperature close to the one used in this work. It should be stressed that since the partition constants depend on the mean occupation number of the quencher in the lipid structure, the ones corresponding to the lower occupation numbers were used. Incorporation of the ASL, CSL, and 12-PCSL was considered to be quantitative. For the lipid molar volume the value $\gamma_L = 0.95 \text{ dm}^3 \text{ mol}^{-1}$ was used, as estimated from published data (33, 34). The values for $[Q]_L$ were also corrected for the dilution effect due to the quencher incorporation. (iii) Blank intensity corrections. Fluorescence intensities in the absence (F_0) and the presence (F) of quencher were corrected by subtracting intensities measured upon injection of an equivalent amount of the ethanol solution according to Equation 3,

$$(F_0/F)_{\text{corr}} = 1/(1 - (F_0/F)_{\text{ethanol}} + (F_0/F)_Q) \quad (\text{Eq. 3})$$

From the fluorescence quenching data, Stern-Volmer plots were obtained according to Equation 4,

$$(F_0/F) = 1 + K_{\text{sv}}[Q]_L \quad (\text{Eq. 4})$$

where F_0 and F correspond to the fluorescence emission of pyrene-labeled AChR or transmembrane fragments in the absence and presence of spin-labeled lipids and $[Q]$ is the concentration of the quencher. Plots of F_0/F versus $[Q]$ yield a slope equal to K_{sv} , the Stern-Volmer constant, *i.e.* the product of the bimolecular rate constant k_q and the fluorophore lifetime (τ) (dynamic mechanism), which was considered invariant for all the fragments. K_{sv} is a measure of the quencher concentration in the fluorophore vicinity, which allowed us to obtain topological information on the labeled cysteine transverse location. Any contribution from static quenching does not hamper the conclusions regarding the topography of the cysteine with respect to the membrane bilayer, as dealt with in a previous publication (31).

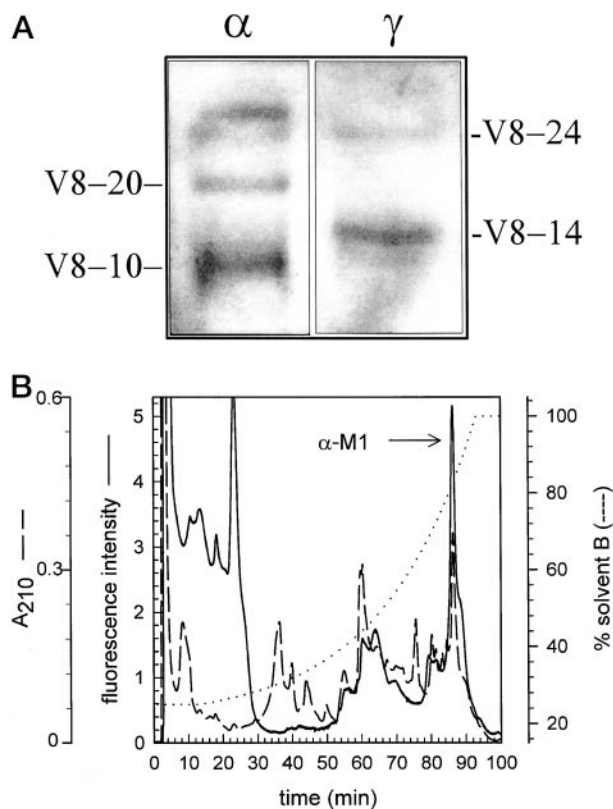


FIG. 1. Proteolytic mapping of the sites of PM reaction on the AChR α - and γ -subunits using *Saccharomyces aureus* V8 protease (A) and reverse-phase HPLC purification α M1-containing fragment (B). A, AChRs reacted with PM were affinity purified and reconstituted into lipid vesicles. Approximately 25 μg of PM-labeled AChRs were resolved by SDS-PAGE on an 8% polyacrylamide slab gel. Following electrophoresis the principal fluorescent bands, the α - and γ -subunit, were visualized on a ultraviolet light box (365 nm) and excised. The excised subunit bands were transferred to the wells of a 15% mapping gel, overlaid with 4 μg of *S. aureus* V8 protease, and electrophoresed (15). Shown is the fluorogram of the mapping gel as viewed on the ultraviolet light box. The mapping gel was then stained with Coomassie Blue and the corresponding fluorescent bands identified from the well established V8 protease pattern of each AChR subunit (15). B, reverse-phase HPLC purification α M1-containing fragment from a tryptic digest of α -V8-20 (Ser¹⁷³-Glu³³⁸) labeled with PM, prepared and purified as described under "Experimental Procedures." The elution profile from an Aquapore C4 reverse-phase HPLC is shown. The elution of the labeled peptide was monitored by absorbance at 210 nm (dashed line) and by fluorescence emission (350 nm excitation; 400 nm emission) (solid line).

RESULTS

Labeling of the Intact AChR and Transmembrane Fragments by PM—For labeling of the intact AChR at free cysteine residues, the AChR was solubilized from *T. californica* AChR-rich membranes in 1% sodium cholate and allowed to react with PM (2 mM) for 1 h. The PM-labeled AChR was then affinity purified and reconstituted into asolectin lipid vesicles (see "Experimental Procedures"). SDS-PAGE of PM-labeled AChRs showed that the majority of the fluorescence is localized in the α - and γ -subunits. The fluorescence was further mapped to large proteolytic fragments of the α - and γ -subunits: α -V8-20 (Ser¹⁷³-Glu³³⁸), α -V8-10 (Asn³³⁹-Gly⁴³⁷), γ -V8-24 (Ala¹⁶⁷-Glu³⁷²), and γ -V8-14 (Leu³⁷³-Pro⁴⁸⁹) (Fig. 1A). In the fragment α -V8-10 there are only two cysteine residues, Cys⁴¹² and Cys⁴¹⁸, both of which are located in the transmembrane segment M4. In α -V8-20 there are three cysteine residue, Cys²²² in the transmembrane segment M1 and Cys¹⁹² and Cys¹⁹³ which are located extracellularly and contribute to the agonist recognition site. In the intact AChR, Cys¹⁹² and Cys¹⁹³ form a vicinal

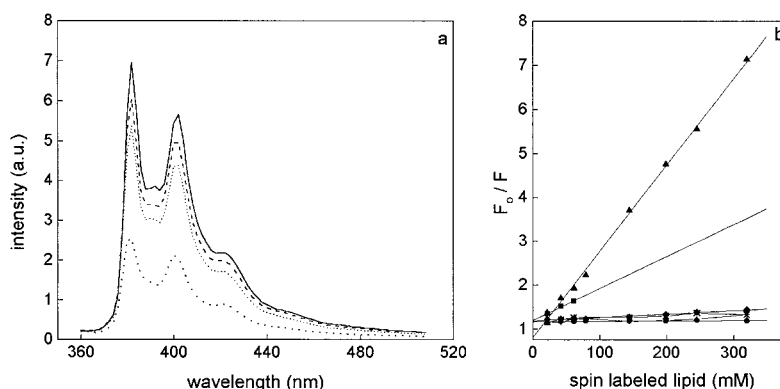


FIG. 2. *a*, Fluorescence spectra of 1-pyrenemaleimide-labeled AChR before (solid line) and after quenching by nitroxide spin-labeled stearic acid analogs (5-SASL, close dots; 7-SASL, spaced dots; 12-SASL, hyphens). *b*, F_0 and F correspond to the fluorescence emission of the PM-labeled AChR in the absence and presence of spin-labeled lipids 5-SASL (\blacktriangle), 7-SASL (Δ), 12-SASL (\circ), ASL (\blacksquare), CSL (\bullet), 12-PC-SL (\blacklozenge), respectively (excitation: 345 nm; emission: 382 nm). A control with addition of ethanol alone was performed in each case (dotted line and + symbols).

disulfide bond leaving Cys²²² as the site of reaction with PM.

The ability of PM-labeled AChRs to undergo agonist-induced state transitions was tested by measuring the agonist sensitivity of the AChR with the hydrophobic photoreactive probe [¹²⁵I]TID. The extent of [¹²⁵I]TID photoincorporation into AChR subunits is ~10-fold greater in the resting state AChR than in the desensitized state, and in the resting state the extent of [¹²⁵I]TID incorporation into the γ -subunit is ~4-fold greater than that into the α -, β -, or δ -subunit (22–23). For PM-labeled AChRs we also found a greater extent of [¹²⁵I]TID incorporation into the γ -subunit relative to the other subunits and the addition of agonist results in a substantial reduction of subunit labeling, indicating that labeled AChRs retain the ability to undergo agonist-induced state transitions (data not shown).

Peptides containing the TM segments α M1 (Ile²¹⁰-Lys²⁴²), α M4 (Tyr⁴⁰¹-Arg⁴²⁹), γ M1 (Lys²¹⁸-Lys²⁵¹), and γ M4 (Val⁴⁴⁶-Arg⁴⁸⁵) were isolated from proteolytic digests and receptor subunits and their identity confirmed by amino-terminal sequence analysis (15) (see Scheme II).

Peptides were labeled with PM and purified by reverse-phase HPLC. Fig. 1B shows the reverse-phase HPLC elution profile of the fragment α Ile²¹⁰-Lys²⁴², which contains the transmembrane segment α M1. Peak HPLC fractions (arrow) were pooled, the solvent removed, the peptide resuspended in detergent (octyl- β -glucoside) and reconstituted into asolectin lipid vesicles.

Quenching of Whole PM-labeled AChR Reconstituted into Asolectin Vesicles by Spin-labeled Lipid Analogs—The fluorescence spectrum of whole PM-labeled AChR reconstituted into asolectin vesicles consisted of only pyrenyl monomer emission (Fig. 2*a*). The extrinsic fluorescence of pyrene-labeled AChR was quenched with three different types of nitroxide spin-labeled lipid analogs: (a) 12-PCSL; (b) the CSL and ASL, with the nitroxide group at carbon 3; and (c) spin-labeled stearic acid analogs, with the nitroxide group at positions 5, 7, and 12 along the acyl chain (5-SASL, 7-SASL, and 12-SASL).

Fig. 2*b* depicts the Stern-Volmer plot of whole AChR quenching by spin-labeled lipid analogs. No deviation from linearity is apparent, and the data were therefore not fitted to a model assuming a fraction of non-accessible fluorophores (e.g. Ref. 35). The Stern-Volmer constants K_{SV} are given in Table I.

It is apparent that 5-SASL and ASL were the most effective quenchers of the pyrene fluorescence of whole AChR reconstituted into asolectin vesicles. In the case of spin-labeled stearic acid derivatives, the 5-SASL isomer quenched more effectively than the 7-SASL and the 12-SASL analogs (Table I), indicating a superficial location of the cysteine-bound pyrenes.

Quenching of Asolectin-reconstituted PM-labeled AChR

Transmembrane Peptide Fragments—PM-labeled AChR TM peptides (see Scheme II) were reconstituted into asolectin vesicles and studied by fluorescence spectroscopy. Upon excitation at 345 nm, pyrenyl monomer emission with maxima at 382 and 402 nm was observed in all cases (Fig. 3). For the γ M4 fragment, an additional weak emission from the single tryptophan residue (Trp⁴⁵³) was observed upon excitation at a wavelength corresponding to intrinsic fluorescence ($\lambda_{exc} = 280$ nm, not shown). Although α M4 possesses two cysteine residues, and hence two potential pyrene tags, pyrenyl emission was not observed to be any stronger with this TM fragment, nor was there any indication of pyrenyl excimer emission ($\lambda_{em} = 480$ nm).

Upon addition of the quenchers, a decrease in intensity was observed in all cases (Fig. 4 and Table I). As is observed for α M4 in Fig. 4, the Stern-Volmer plot shows a linear dependence. The two cysteines in α M4 are several residues apart, and are thus likely to exhibit different accessibility to the quenchers. If the two Cys residues had reacted with PM, a deviation from linearity would result; this is not the case (Fig. 4). Thus, of the two potential tags only a single cysteine in α M4 appears to have reacted to any significant extent (Cys⁴¹² or Cys⁴¹⁸). Furthermore, and on the basis of previous studies showing that Cys⁴¹² exhibits a preferential reactivity to structurally diverse hydrophobic probes (15), it is likely that Cys⁴¹² is the residue labeled with pyrene in α M4. Quenching of the pyrenyl fluorescence in the other TM fragments followed the same pattern as that of α M4.

The use of a families of nitroxide spin-labeled analogs having known graded series of depths in the membrane has set the experimental basis (30, 32, 36–39) for the well established differential quenching methodologies. From inspection of Table I it can be concluded that the fluorophore is in all cases very close to the membrane-water interface: quenching is highest for 5-SASL, much lower, similar values are obtained for 7-SASL and 12-SASL. The very high value of 5-SASL compared with the nearby located 7-SASL points to a very specific location of the former at a shallow position in the membrane.

The quenching efficiency for CSL was determined for the γ M4 fragment (Table I). The absolute value of the Stern-Volmer constant is very low, and much lower than that obtained for a similar steroid (ASL), pointing to a preferential distribution of the latter in the vicinity of the peptide (cf. Table I).

DISCUSSION

This work constitutes the first study comparing the topography of whole AChR and four constituent TM fragments with

TABLE I
Stern-Volmer constants (K_{SV}), for the quenching of pyrene labeled transmembrane fragments and whole AChR by spin-labeled positional isomers of fatty acids, phosphatidylcholine, and the steroids cholestane and androstane

K_{SV} M^{-1}	Whole AChR	α -M1	γ -M1	α -M4	γ -M4
5-SASL	9.87 ± 1.09	6.59 ± 0.48	7.75 ± 0.25	11.44 ± 1.29	12.79 ± 1.45
7-SASL	1.82 ± 0.07	1.46 ± 0.09	2.07 ± 0.14	1.38 ± 0.08	1.83 ± 0.07
12-SASL	1.88 ± 0.04	1.14 ± 0.33	2.09 ± 0.12	1.45 ± 0.02	2.46 ± 0.25
12-PCSL	0.78 ± 0.05				
CSL	0.21 ± 0.07				0.39 ± 0.06
ASL	3.16 ± 1.00	2.75 ± 0.41	3.43 ± 0.38	2.55 ± 0.27	3.59 ± 0.58

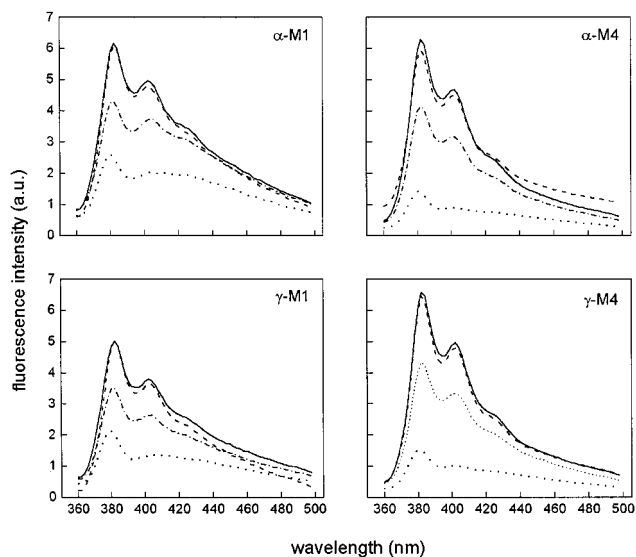


FIG. 3. Fluorescence spectra of PM-labeled AChR fragments reconstituted in asolectin and their quenching by nitroxide spin-labeled analogs. Excitation wavelength, 345 nm. Spectra are shown before (—) and after addition of $8 \mu M$ of the following nitroxide spin-labeled lipids: 5-SASL (small dots), 12-SASL (hyphens), and CSL (dashes).

respect to the membrane framework. Use was made of the extrinsic fluorescence of pyrene, a probe having advantageous properties for studying the structure and dynamics of proteins. For this reason, we introduced pyrenyl ligands for the study of proteins in living cholinergic synapses (40) and pyrene adducts have been successfully used to label purified AChR (21, 27, 30, 41). Here, we obtained relevant structural information using differential quenching of pyrene-labeled AChR and constituent peptides by fatty acid, phospholipid, and steroid spin labels. These probes, having nitroxide groups at different positions, act as molecular rulers that enabled us to learn about the spatial relationship between the pyrene-labeled AChR TM domains and the membrane bilayer.

In their previous study of isolated AChR fragments, Corbin *et al.* (17) were aware that their structural specificities might not reflect those of the whole AChR. Here we present experimental evidence showing that the same topological pattern is obtained for reconstituted whole AChR and derived transmembrane peptides, thus validating the inferences made on the intact receptor topology from studies using lipid-reconstituted peptides.

Quenching of PM-labeled AChR—The extrinsic fluorescence of the intact, pyrene-labeled AChR was more readily accessible to quenching by 5-SASL and ASL than by PC or cholestane analogs (Table I). The quenching efficiency (K_{SV}) of the whole AChR with the phospholipid spin-labeled 12-PCSL was much lower than with the equivalent fatty acid probe, 12-SASL (*cf.* Table I). If we assume there is no significant variation in nitroxide moiety between the two probes, this means that the

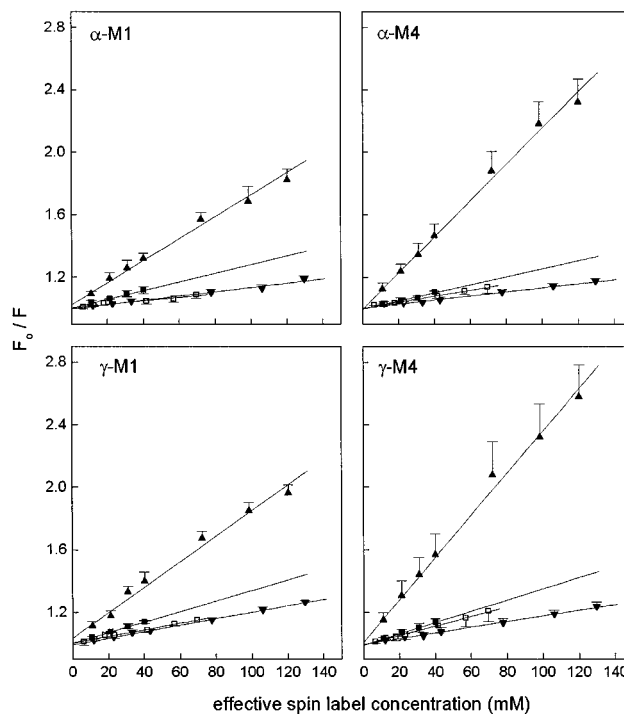


FIG. 4. Stern-Volmer plot of the quenching of PM-labeled AChR transmembrane fragments by the nitroxide spin-labeled analogs 5-SASL (\blacktriangle), 7-SASL (\blacktriangledown), 12-SASL (\square), and ASL (\blacksquare). F_0 and F correspond to the fluorescence emission in the absence and presence of spin-labeled lipids, respectively (excitation: 345 nm; emission: 382 nm).

fatty acid analog exhibits a stronger affinity than the PC analog for the peptide, in agreement with previous experimental work (42, 43). Alternatively, the difference in K_{SV} may reflect differences in the topography of fatty acid and phospholipid sites.

Quenching of PM-labeled AChR TM Segments Reconstituted in Asolectin Liposomes—The weak Trp⁴⁵³ emission in the γ M4 fragment upon excitation at its absorption maximum ($\lambda_{exc} = 280$ nm) is most likely due to an efficient energy transfer to the nearby pyrene in Cys⁴⁵¹. This assumption was used previously to calculate the Cys⁴⁵¹-Trp⁴⁵³ inter-residue distance of 18 Å on the basis of a Förster radius of 20 Å (30). A major finding of the present work is that pyrene-labeled Cys residues lie near the lipid-water interface in whole AChR and all receptor-derived fragments studied. This is to be analyzed in the light of current models on the possible secondary structure and topological disposition of AChR transmembrane regions. A refined theoretical prediction of AChR secondary structure was recently reported (44). The TM segments are predicted to be in a mixed α/β form, with a stronger contribution from α -helices. The precise length of the segments in the membrane is described as “poorly accurate.” In addition, no information about the orientation of the TM domains in the bilayer could be obtained,

except for the M2 segment, which appears to lie perpendicular to the membrane.

The quenching data for the M4 fragments is compatible with a rather shallow location of the label, occurring on Cys⁴¹² at α M4 and on Cys⁴⁵¹ at γ M4. In previous quenching studies of whole AChR labeled with PM at γ M4 Cys⁴⁵¹, K_{sv} values of 0.19 and 0.07 were reported for 5-SASL and 12-SASL, respectively (30). In agreement with the findings of the present work, these authors concluded that the pyrene-labeled residue was at a superficial location in the membrane. However, since data were not corrected for the different partition coefficient of the two fatty acids or for the effective concentration in the membrane volume, the K_{sv} values obtained cannot be compared with each other. These results are compatible with an α -helical configuration of the TM regions involved, as these specific labeled residues are localized at the beginning of the TM region of the fragments (see Scheme II).

We have recently obtained complementary information about the structure of γ M4 using magic-angle NMR spectroscopy and wideline NMR of oriented bilayers. γ M4 was prepared by solid-state synthesis and reconstituted in L- α -dimyristoylphosphatidylcholine lipid bilayers. Heteronuclear dipolar recoupling NMR suggests the distance between Leu⁴⁵⁸ and Gly⁴⁶² to be less than 5 Å, which is consistent with a helical structure of γ M4 (19). Orientational constraints obtained from wideline NMR of oriented bilayers ("bicelles") indicate that this TM domain adopts a tilted orientation relative to the bilayer normal (19).

The quenching data for the α M1 fragment is compatible with a rather shallow location of the labeled Cys²²². If α M1 were a linear helix perpendicular to the membrane surface, Cys²²² should be located at the center of the hydrophobic stretch (see Scheme II). In recent work (21), data for the whole AChR under conditions in which α M1 Cys²²² was labeled with PM were interpreted to mean a shallow location of the pyrene moiety, close to the membrane-water interface. Assuming a membrane thickness of \sim 30 Å and the observation that the nitroxide group in 5-SASL is located 11.5 Å away from the membrane center, estimated from the known values for 6-anthroxly stearic acid (10.9 Å, Ref. 37), and 5-PCSL (12.15 Å, Ref. 38), if M1 were a straight helix it ought to lie at an angle of \sim 13° with respect to the membrane plane, *i.e.* practically "adsorbed" at the interface, an altogether very unlikely contention. In addition, it should be stressed that the conclusions obtained for the structure of α M1 are not due to any perturbation introduced by the pyrene probe, since the same pattern was obtained in another experiment in which the cysteine residue was derivatized with a different probe, a nitroxide spin label (21).

The behavior of α M1 may be due to the occurrence of three Pro residues along the stretch, one of them (Pro²²¹) immediately adjacent to Cys²²². Proline residues are known to introduce torsions of about 26° in a helix, because they eliminate backbone hydrogen bonds (45). This backbone distortion also occurs in transmembrane α -helices (46), and is a likely rationale for explaining the experimental data on the proline-rich α M1 domain. This AChR region is therefore very unlikely to be a straight α -helix, although recent preliminary NMR data on an α M1-containing recombinant fragment indicate a predominantly α -helical secondary structure (47).

In the work of Blanton and Cohen (14), four residues in *Torpedo* α M1 (Cys²²², Leu²²³, Phe²²⁷, and Leu²²⁸) were labeled with a lipophilic photoreactive probe, and thus are believed to be in contact with or directly accessible from the membrane. This pattern is not compatible with either α -helix or β -sheet alone. Also, CD and FTIR studies indicate substantial amounts of non-helical structure in α M1 (17). Ortells and Lunt (48) in

their mixed α -helix/ β -sheet model of the AChR, constructed α M1 as a three-strand β -sheet and introduced short loops generated by searching in the data base of known structures for an appropriate backbone conformation. The proline residues themselves cannot be found within a β -strand, so they were positioned in the loops. The same explanation can be extended to γ M1, having a proline residue (Pro²²⁹) immediately adjacent to Cys²³⁰ and two other (Pro²²² and Pro²⁴⁴) at the end of the TM region (see Scheme II). Thus, the conserved proline residues in M1 segment might introduce "curls" or kinks in a manner analogous to that recently reported for one of the transmembrane segments of the K⁺ channel (49). In the case of the γ M1 fragment there appears to be no detailed information on its topography in the membrane as yet.

Relative Affinities of Spin Label Lipid Analogs for the Whole AChR and Derived TM Segments—Experimental data obtained in the present work can be further exploited to extract information about the relative affinity of spin-labeled lipids for the whole *T. californica* AChR and TM AChR peptides. For this purpose one should compare the relative quenching efficiencies for probes located at the same depth in the membrane. In this way, variations in K_{sv} are not due to the specific topography, but reflect the relative affinities of the probe. There is scant information in the literature on the location of the sterols androstane and cholestane in a membrane. The former shows structural resemblance to 22-(N-(7-nitrobenz-2-oxa-1,3-diazol-4-yl)amino)-23,24-bisnor-5-cholen-3 β -ol-cholesterol; their hydroxyl groups are similarly held by the rigid heterocyclic moieties. If the distance of \sim 5.7 Å from the center of the bilayer measured for NBD-cholesterol (38) is extrapolated to the location of the nitroxide group in ASL, it follows that this is about the same as that of 12-SASL. In contrast, the hydroxyl group is substituted by a hydrophobic alkyl chain in the case of CSL, resulting in a more shallow location of the nitroxide spin label, close to that of 5-SASL, in agreement with the ESR isotropic hyperfine splitting factor measurements and the rates of reduction of these probes incorporated into membranes (50).

As shown in Table I, the Stern-Volmer constant for γ M4 quenching is much larger for 5-SASL than for CSL. Thus, CSL does not exhibit the strong selectivity for the isolated transmembrane γ M4 region shown by fatty acids or androstane, in agreement with previous ESR data on native AChR-rich membranes (51). Let us assume that the local quencher concentration at each membrane depth $[Q]$, is related to the overall concentration in the membrane $[Q]_L$ by Equation 5 (31),

$$[Q] = \beta[Q]_L \quad (\text{Eq. 5})$$

where the factor β is introduced to account for the fact that the quencher molecules in the bilayer volume are not homogeneously distributed relative to the fluorophore. From Equation 5 the resulting relative affinities for the pairs 5-SASL:CSL and 12-SASL:ASL are 9:1 and 0.7:1, respectively. These apparent affinities are to be treated with caution, especially in view of the fact that for these sterol molar concentrations phase separation might occur (52). The same reasoning should be applied to the whole AChR quenching data, where relative affinities for ASL > 12-PCSL are observed, in this case with a ratio 7:1.

Conclusions—The differential fluorescence quenching by spin-labeled lipids of whole AChR and transmembrane fragments derivatized in Cys residues with *N*-(1-pyrenyl)maleimide shows in all cases a superficial location of the chromophore. This is as expected for the α M4 and γ M4 fragments, but not so for the M1 segments, in which case "classical" models locate Cys residues at the center of the bilayer. The topography emerging from the fluorescence data can be rationalized, however, on the basis of a substantial amount of non-helical struc-

ture, attributable to the occurrence of proline residues, which are known to introduce kinks in α -helices. M1 exhibits the fixed presence of conserved proline residues, not only in the AChR but also in all ligand-gated ion channels (48). Thus the data is compatible with either non-linear α -helices or pleated β structures in M1. Further studies using other methodologies are needed to clarify the topography of the transmembrane α M1 segment.

Another important conclusion from the present work is that fatty acid and androstane spin labels exhibit a higher affinity for AChR and derived TM peptides than do spin-labeled phosphatidylcholine and cholestane. This reinforces the view that AChR possesses selectivity for certain lipid species, in agreement with previous results (42, 51). Interestingly, the behavior found for the whole reconstituted AChR is the same as for the peptides, showing that the latter reflect quite faithfully the properties of the parental molecule.

REFERENCES

- Smith, G. B. & Olsen, R. W. (1995) *Trends Pharmacol. Sci.* **16**, 162–168
- Jackson, M. B. & Yakel, J. L. (1995) *Annu. Rev. Physiol.* **57**, 447–468
- Kuhse, J., Betz, H. & Kirsch, J. (1995) *Curr. Opin. Neurobiol.* **5**, 318–323
- Changeux, J. P. & Edelman, S. J. (1998) *Neuron* **21**, 959–980
- Barrantes, F. J. (1998) *The Nicotinic Acetylcholine Receptor: Current Views and Future Trends*, Springer Verlag, Berlin/Heidelberg and Landes Publishing Co., Georgetown, TX
- Blanton, M. P. & Cohen, J. B. (1992) *Biochemistry* **31**, 3738–3750
- Chavez, R. A. & Hall, Z. W. (1992) *J. Cell Biol.* **116**, 385–393
- Noda, M., Takahashi, H., Tanaba, T., Toyosato, M., Kikuyotani, S., Furutani, Y., Hirose, T., Takashima, H., Inayama, S., Miyata, T. & Numa, S. (1983) *Nature* **302**, 528–532
- Unwin, N. (1993) *J. Mol. Biol.* **229**, 1101–1124
- Unwin, N. (1995) *Nature* **373**, 37–43
- Ortells, M. O., Barrantes, G. E. & Barrantes, F. J. (1998) in *The Nicotinic Acetylcholine Receptor: Current Views and Future Trends*, Barrantes, F. J., ed, pp. 85–108, Springer Verlag, Berlin/Heidelberg and Landes Publishing Co., Georgetown
- Opella, S. J., Marassi, F. M., Gesell, J. J., Valente, A. P., Kim, Y., Oblatt-Montal, M. & Montal, M. (1999) *Nature Struct. Biol.* **6**, 374–379
- Pashkov, V. S., Maslennikov, I. V., Tchikin, L. D., Efremov, R. G., Ivanov, V. T. & Arseniev, A. S. (1999) *FEBS Lett.* **457**, 117–121
- Blanton, M. P. & Cohen, J. B. (1994) *Biochemistry* **33**, 2859–2872
- Blanton, M. P., McCardy, E. A., Huggins, A. & Parikh, D. (1998) *Biochemistry* **37**, 14545–14555
- Baenziger, J. E. & Méthot, N. (1996) *J. Biol. Chem.* **270**, 29129–29137
- Corbin, J., Méthot, N., Wang, H. H., Baenziger, J. E. & Blanton, M. P. (1998) *J. Biol. Chem.* **273**, 771–777
- Lugovskoy, A. A., Maslennikov, I. V., Utkin, Y. N., Tsetlin, V. I., Cohen, J. B. & Arseniev, A. S. (1998) *Eur. J. Biochem.* **255**, 455–461
- Williamson, P. F., Bonev, B., Barrantes, F. J. & Watts, A. (2000) *Biophys. J.* **78**, 147A
- Akabas, M. H. & Karlin, A. (1995) *Biochemistry* **34**, 12496–12500
- Kim, J. & McNamee, M. G. (1998) *Biochemistry* **37**, 4680–4686
- Sobel, A., Weber, M. & Changeux, J. P. (1977) *Eur. J. Biochem.* **80**, 215–224
- Pedersen, S. E., Dreyer, E. B. & Cohen, J. B. (1986) *J. Biol. Chem.* **261**, 13735–13743
- Ellena, J. F., Blazing, M. A. & McNamee, M. (1983) *Biochemistry* **22**, 5523–5535
- Blanton, M. P. & Wang, H. H. (1991) *Biochim. Biophys. Acta* **1067**, 1–8
- White, B. H., Howard, S., Cohen, S. G. & Cohen, J. B. (1991) *J. Biol. Chem.* **266**, 21595–21607
- Blanton, M. P., McCardy, E. A. & Gallagher, M. J. (2000) *J. Biol. Chem.* **275**, 3469–3478
- Schagger, H. & von-Jagow, G. (1987) *Anal. Biochem.* **166**, 368–379
- Green, S. A., Simpson, D. J., Zhou, G., Ho, P. S. & Blough, N. V. (1990) *J. Am. Chem. Soc.* **112**, 7337–7346
- Narayanaswami, V., Kim, J. & McNamee, M. G. (1993) *Biochemistry* **32**, 12413–12419
- Castanho, M., Prieto, M. & Acuña, A. U. (1996) *Biochim. Biophys. Acta* **1279**, 164–168
- Blatt, E., Chatelier, R. C. & Saywer, W. H. (1984) *Photochem. Photobiol.* **39**, 477–483
- Cornell, B. A. & Separovic, F. (1983) *Biochim. Biophys. Acta* **733**, 189–193
- Lewis, B. A. & Engelman, D. M. (1983) *J. Mol. Biol.* **166**, 211–217
- Lehrer, S. S. (1971) *Biochemistry* **10**, 3254–3263
- Chattopadhyay, A. (1992) in *Biomembrane Structure and Function: The State of the Art* (Gaber, B. P., and Easwaran, K. R. K., eds) pp. 153–163, Adenine Press, Schenectady, NY
- Abrams, F. S., Chattopadhyay, A. & London, E. (1992) *Biochemistry* **31**, 5322–5327
- Chattopadhyay, A. & London, E. (1987) *Biochemistry* **26**, 39–45
- Ladokhin, A. S. (1999) *Biophys. J.* **76**, 946–955
- Barrantes, F. J., Sakmann, B., Bonner, R., Eibl, H. & Jovin, T. M. (1975) *Proc. Natl. Acad. Sci. U. S. A.* **72**, 3097–4001
- Marquez, J., Iriarte, A. & Martinez-Carrion, M. (1989) *Biochemistry* **28**, 7433–7439
- Marsh, D. & Barrantes, F. J. (1978) *Proc. Natl. Acad. Sci. U. S. A.* **75**, 4329–4333
- Barrantes, F. J. (1978) *J. Mol. Biol.* **124**, 1–26
- Le Novère, N., Corringer, P.-J. & Changeux, J.-P. (1999) *Biophys. J.* **76**, 2329–2345
- MacArthur, M. W. & Thornton, J. M. (1991) *J. Mol. Biol.* **218**, 397–412
- von Heijne, G. (1991) *J. Mol. Biol.* **218**, 499–503
- Grant, M. A., Gentile, L. N., Shi, Q.-L. & Hawrot, E. (1999) *Biochemistry* **38**, 19730–10742
- Ortells, M. O. & Lunt, G. G. (1996) *Protein Eng.* **9**, 51–59
- del Camino, D., Holmgren, M., Liu, Y. & Yellen, G. (2000) *Nature* **403**, 321–325
- Schreier-Muccillo, S., Marsh, D. & Smith, I. C. P. (1976) *Arch. Biochem. Biophys.* **172**, 1–11
- Arias, H. R., Sankaram, M. B., Marsh, D. & Barrantes, F. J. (1990) *Biochim. Biophys. Acta* **1027**, 287–294
- Schroeder, F., Jefferson, J. R., Kier, A. B., Knittel, J., Scallen, T. J., Wood, W. G. & Hapala, I. (1991) *Proc. Soc. Exp. Biol. Med.* **196**, 235–252